

K1 Capsule-dependent phage-driven evolution in *Escherichia coli* leading to phage resistance and biofilm production

Céline Antoine ^{1,2}, Fanny Laforêt ^{1,2}, Abdoulaye Fall ^{3,#}, Bob Blasdel ⁴, Véronique Delcenserie ^{2,†} and Damien Thiry ^{1,†,*}

¹ Veterinary bacteriology, Department of Infectious and Parasitic Diseases, FARAH and Faculty of Veterinary Medicine, ULiège, 4000 Liège, Belgium; celine.antoine@uliege.be, fanny.laforet@uliege.be, damien.thiry@uliege.be

² Food Science Department, FARAH and Faculty of Veterinary Medicine, ULiège, 4000 Liège, Belgium; veronique.delcenserie@uliege.be

³ FoodChain ID GENOMICS SA, Herstal, Belgium, abdoulaye.fall@foodchainid.com

⁴Vésale Bioscience, Vésale Pharmaceutica, Noville-sur-Mehaigne, Belgium ; bob.blasdel@phage.health

[#]This author no longer works at this address.

[†] These authors equally supervised the work

^{*} Corresponding author: Damien Thiry. E-mail address: Damien.thiry@uliege.be Tel.: +32-4-3669522

23 Abstract

24 *Aims:* Understanding bacterial phage resistance mechanisms has implications for developing phage-
25 based therapies. This study aimed to explore the development of phage resistance in *Escherichia coli*
26 K1 isolates' to K1-ULINTec4, a K1-dependent bacteriophage.

27 *Methods and results:* Resistant colonies were isolated from two different strains (APEC 45 and C5),
28 both previously exposed to K1-ULINTec4. Genome analysis and several parameters were assessed,
29 including growth capacity, phage adsorption, phenotypic impact at capsular level, biofilm production
30 and virulence in the in-vivo *Galleria mellonella* larvae model. One out of the 6 resistant isolates
31 exhibited a significantly slower growth rate suggesting the presence of a resistance mechanism altering
32 its fitness. Comparative genomic analysis revealed insertion sequences in the region 2 of the *kps* gene
33 cluster involved in the capsule biosynthesis. In addition, an immunoassay targeting the K1 capsule
34 showed a very low positive reaction compared to the control. Nevertheless, microscopic images of
35 resistant strains revealed the presence of capsules with a clustered organization of bacterial cells and
36 biofilm assessment showed an increased biofilm production compared to the sensitive strains. In the
37 *G. mellonella* model, larvae infected with phage-resistant isolates showed better survival rates than
38 larvae infected with phage-sensitive strains.

39 *Conclusions:* A phage resistance mechanism was identified at the genomic level and had a negative
40 impact on the K1 capsule production. The resistant isolates showed an increased biofilm production,
41 and a decreased virulence in vivo.

42 *Impact statement:* This study describes the implications of *E. coli* K1 resistance development against
43 phage K1-ULINTec4. The in-vivo virulence decrease was nevertheless accompanied by an increase in
44 biofilm formation observed among resistant isolates. This raises concerns for K1-dependent phages
45 use in some pathologies.

46
47 **Keywords:** phage resistance; *Escherichia coli* K1, capsule-dependent phage, *Galleria mellonella*,
48 genome analysis, biofilm

49 1. Introduction

50 *Escherichia coli* K1 belongs to the pathotype of extraintestinal *E. coli* as it displays specific features
51 and virulence factors that allows it to develop and survive outside the gastrointestinal tract (Dale and
52 Woodford 2015). Among these factors, the K1 capsule plays an essential role in evading the host
53 immune system by providing protection against phagocytosis and complement-mediated killing, thus
54 promoting bacterial survival (Sarowska et al. 2019). *E. coli* K1 is associated with urinary tract
55 infections, sepsis and with neonatal meningitis, a potentially fatal infection that mainly affects
56 premature newborns that can be transmitted horizontally from mother to child (Kim 2017, King et al.
57 2015, McCarthy et al. 2016). The commensal presence of these bacteria in the adult gut microbiota
58 allows for their transmission during childbirth, leading to colonization of the newborn's
59 gastrointestinal tract and subsequent translocation into the circulatory system (McCarthy, Birchenough
60 and Taylor 2019). They are also responsible for pathologies in animals, particularly colibacillosis in
61 poultry, with the predominant serotypes O1, O2, O18 and O45. These serotypes are also common in *E.*
62 *coli* K1 involved in neonatal meningitis, sepsis and urinary tract infections in humans (Kim 2017,
63 King et al. 2015, Dziva and Stevens 2008, Mora et al. 2013, Moulin-Schouleur et al. 2006). *E. coli*
64 O18:K1:H7 isolated from human and chicken extra-intestinal infections share many similarities and
65 are able to induce colibacillosis in chicks (Moulin-Schouleur et al. 2006). In addition, one study
66 revealed the prevalence of O45:K1:H7-B2-ST95 strains sharing genetic and virulence characteristics
67 between poultry and humans (Mora et al. 2013).

68 Neonatal meningitis represents a critical threat to newborns, with potentially fatal consequences. In
69 addition, shared features between human infections and poultry colibacillosis highlight the potential
70 for zoonotic transmission (Kim 2017, Mora et al. 2013). Therefore, the development of new treatment
71 strategies is necessary. With renewed interest in the global threat of bacterial resistance to antibiotics,
72 phage therapy is one of the most promising approaches. Lytic bacteriophages play an essential role in
73 the complex interaction between *E. coli* K1 and its environment. They can be classified into two main
74 categories: capsule-dependent and capsule-independent K1 phages (Bull, Vimr and Molineux 2008).

75 Capsule-independent K1 phages are not influenced by the presence of the capsule and can infect *E.*

76 *coli* K1 independently of this feature. Conversely, capsule-dependent K1 phages have an affinity for
77 the polysaccharidic capsule and are able to degrade polysialic acid using specific enzymes called
78 endosialidases (Bull, Vimr and Molineux 2008, Leiman et al. 2007, Scholl et al. 2001). Several studies
79 have evaluated the therapeutic potential of these phages in the treatment of various infections, with
80 encouraging results (Antoine et al. 2021, Møller-Olsen et al. 2018, Schneider et al. 2018, Smith and
81 Huggins 1982).

82 The understanding of the bacterial phage resistance mechanisms has implications for the development
83 of molecular models of cell surface moieties, tools for bacterial engineering, and phage-based
84 therapeutic strategies. The arms race between bacteria and phages has led to the development of
85 diverse and complex resistance mechanisms within bacterial populations (Azam and Tanji 2019).
86 These mechanisms can be divided into three groups: receptor adaptations, host defense systems and
87 phage-derived phage defense systems (Egido et al. 2022). In the first case, bacteria use strategies to
88 suppress phage adsorption. A common mechanism involve point mutations, which can lead to
89 modification of receptor structure or a suppression of receptor expression (Burmeister et al. 2020,
90 Chapman-McQuiston and Wu 2008, Kim et al. 2015). In response to phage infection, some bacteria
91 can also produce proteins that block or mask the receptor or can employ phase variation (Seed et al.
92 2012, Gencay et al. 2018). If these changes occur in receptors involved in bacterial survival or
93 virulence, the host's bacterial fitness may be compromised (Mangalea and Duerkop 2020). The second
94 group covers several phage defense mechanisms targeting viral nucleic acids or leading to abortive
95 infection. It includes the classical (type I-IV) and related (DISARM, BREX, Ago) restriction-
96 modification systems (Egido et al. 2022, Oliveira, Touchon and Rocha 2014, Ofir et al. 2018, Goldfarb
97 et al. 2015, Wu et al. 2020). Another well-known bacterial defense system against mobile genetic
98 elements is the CRISPR-Cas system (Azam and Tanji 2019, Millen et al. 2012). In addition, other
99 systems involved, for example, in abortive infection processes that rely on a variety of genetic
100 functions, such as the toxin-antitoxin mechanism, impose a cost on the infected cell by sacrificing its
101 survival for the collective benefit of the bacterial population (Dy et al. 2014). Several studies have
102 highlighted a wide range of other bacterial defense mechanisms against phages. However, many of

these complex mechanisms are still not fully understood, underscoring the complexity of the field of phage resistance.

Bacterial resistance to phages has already been demonstrated in experiments carried out on *E. coli* K1, with a compensatory reduction in virulence (Antoine et al. 2021, Smith and Huggins 1982). A mechanism of resistance to phage K1F was identified in one *E. coli* K1 laboratory strain with genomic mutations generating phenotypic changes at the capsular level, as well as a fitness cost (Styles et al. 2022). The aim of this study was to investigate the resistance of two clinical *E. coli* K1 strains involved respectively in neonatal meningitis and colibacillosis to the phage K1-ULINTec4. Genomic and phenotypic techniques were used to assess the consequences of this resistance on the bacterial virulence and biofilm production.

2. Materials and Methods

2.1 Bacteriophage and Bacterial Strains

The O18:K1 avian pathogenic strain APEC45 strain was isolated from a turkey in 1995 in France. This isolate was responsible for clinical signs of colibacillosis (Moulin-Schouleur et al. 2006). Strain APEC45 is the isolation and propagation strain of phage K1-ULINTec4 (Antoine et al. 2021). The neonatal meningitis *E. coli* (NMEC) strain C5 "Bort" (O18ac:K1:H7) was isolated in 1975 from cerebrospinal fluid of a newborn. This strain was obtained from the American Type Culture Collection (ATCC) (LGC Standards, Molsheim, France) and is designated as *Escherichia coli* (Migula) Castellani and Chalmers ATCC 700973. C5 was selected because of its human origin and its serotype similar to APEC45. Bacterial cultures were grown in LB Lennox broth at 37 °C. The phage vB_EcoP_K1-ULINTec4 was isolated in 2020 in Liège from wastewater, using the strain APEC45. This K1-dependent phage, classified under the *Vectrevirus* genus, was previously assessed in-vitro and in-vivo (Antoine et al. 2021). This phage produces lysis plaques with a peripheral halo in contact with *E. coli* K1 suggesting the presence of a depolymerase, and its genome encodes an endosialidase.

128

129 **2.2 Isolation of Bacteriophage Resistant Mutants**

130 Phage-resistant mutants were generated by exposing APEC45 and C5 to the phage K1-ULINTec4.
 131 Briefly, 100 μ L of phage (log 9 PFU ml⁻¹) as well as 200 μ L of bacterial culture (OD_{600nm}: 0.2-0.3)
 132 were added to 4 mL of molten LB agar (1mM CaCl₂, 1mM MgSO₄), poured onto LB Lennox agar
 133 plate (1mM CaCl₂, 1mM MgSO₄) and incubated at 37°C for 24h. Three colonies per strain were
 134 harvested and grown in 5 mL of LB broth at 37°C overnight. Half of each culture was stored at -20°C
 135 and -80°C with addition of an equivalent volume of glycerol 80%. Phage resistance was confirmed
 136 using 10 μ L phage spot tests on LB Lennox agar (1mM CaCl₂, 1mM MgSO₄) covered with a bacterial
 137 overlay (OD: 0.2-0.3). The plates were incubated overnight at 37°C before lysis visualization.

138 **2.3 Stability of phage resistance**

139 The stability of resistance in phage resistant isolates was assessed as follows. Each resistant isolate
 140 was cultivated from a single colony in 5 mL of LB Lennox, incubated overnight at 37°C.
 141 Subsequently, ten consecutive passages were conducted, wherein 5 μ L of culture was transferred to 5
 142 mL of LB Lennox, and cultured for 24 hours at 37°C. After each passage, phage spot tests involving
 143 10-fold serial dilutions (ranging from 10³ to 10⁹ PFU ml⁻¹) were performed on LB Lennox agar plates
 144 (1mM CaCl₂, 1mM MgSO₄). These plates were preloaded with 200 μ L of the culture of the resistant
 145 isolate and 4 mL of molten LB agar (1mM CaCl₂, 1mM MgSO₄). The visual assessment of phage
 146 lysis was conducted after a 24-hour incubation at 37°C.

147 **2.4 Bacterial Growth Curves**

148 Growth curves were generated in a 96-well microplate in triplicate. Sensitive and resistant strains were
 149 tested in triplicate without and with the presence of phage K1-ULINTec4. Each well was filled with
 150 180 μ L of LB Lennox, 10 μ L of bacterial culture (LB Lennox, OD: 0.2-0.3) of each of the eight tested
 151 *E. coli* K1 (2 sensitive strains and 6 resistant isolates) and 10 μ L of either PBS or ULINTec4 phage
 152 solution (PBS, log 8 PFU ml⁻¹) reaching an MOI of 1. Readings were performed using an Allsheng
 153 *AMR-100T* automatic 96-well plate reader (Hangzhou Allsheng Instruments Co., Ltd., Hangzhou,

China). The plate was placed at 37°C under constant shaking and readings (630nm) were taken every 30 minutes for 12 hours.

2.5 Bacteriophage Adsorption

The six resistant isolates and the two sensitive strains were grown in 5 mL of LB Lennox broth at 37°C until reaching an optical density of 0.25 (log 8 CFU ml⁻¹) and 990 µL of culture were distributed in three centrifuge tubes per isolate. Then, 10 µL of phages (log 8 PFU ml⁻¹) were added to each culture, reaching a MOI of 0.1, and incubated at 37°C. Samples (10 µL) were taken at 2, 3, 5, 8, 10, 15 and 20 min and immediately diluted in 990 µL of PBS. All samples were then centrifugated (1 min, 20000g) and subsequently titrated in triplicate using ten-fold serial dilutions and spotting of 2µL drops on APEC45 bacterial overlay (OD: 0.2-0.3). The adsorption time was determined as the time when the ratio of non-adsorbed phage (P) over the initial phage number (P₀) was lower than 0.1 (Antoine et al. 2021).

2.6 Detection of K1 antigen

The K1 antigen of *E. coli* was detected by latex agglutination using Wellcogen™ Neisseria meningitidis B/E. coli K1 Rapid Latex Agglutination Test following manufacturer's instructions (Thermoscientific, Waltham, MA, USA). A negative control and a latex control were also performed.

2.7 Capsule detection by optical microscopy

The presence of bacterial capsules was assessed by optical microscopy using the Maneval negative staining technique (Maneval 2009). Bacterial cultures were incubated overnight at 37°C and 10 µL of each culture were mixed with 10 µL of a 1% Congo red solution (Sigma-aldrich, Saint-Louis, MO, USA), spread on a glass slide and air-dried. The slide was then recovered with a Maneval solution (0.05% Acid fuchsin, 3.9% phenol, 2.8% FeCl₃, 4.9% Acetic Acid) for 30 min and then gently washed with demineralized water. Bacteria were observed at 100x magnification using optical microscopy. As the K1 capsule is not expressed at low temperatures, cultures of strains APEC45 and C5 at 18°C were used as negative controls while the same strains cultivated at 37°C were used as positive controls.

2.8 Biofilm production

The biofilm production was assessed based on microscopic observation of bacterial clusters and was performed as follows. A 100x dilution of an overnight culture (LB Lennox) was dispensed into a 96-well plate in 10 x 100 μ L replicates. After 24 h of incubation at 37°C without agitation, the supernatant was removed and 150 μ L of crystal violet 0,1% (Acros Organics, Fair Lawn, NJ, USA) was added for 10 min. The plate was then washed 3 times with PBS and air-dried. The crystal violet was dissolved with 200 μ L of 30% acetic acid for 10 min. After resuspension, a volume of 100 μ L of each well was transferred to a new plate and optical densities were measured at 570 nm using a Benchmark microplate reader (Biorad, Hercules, CA, USA). The OD_{570nm} of a negative control composed of pure medium and undergoing the same conditions as the test samples was subtracted to all measurements. Statistical significance was assessed using one-way ANOVA with Dunnet's multiple comparison test.

2.9 Genome sequencing

The six resistant isolates and the two sensitive strains were genomically sequenced. Total genomic DNA was extracted from 1 ml of the samples using the DNeasy Blood & Tissue kit (Qiagen). DNA was eluted into DNase- and RNase-free water, and concentration and purity were determined using a Nanodrop ND-1000 spectrophotometer (Isogen, St-Pieters-Leeuw, Belgium). DNA QC was performed with a Fragment Analyzer (Agilent) using the High Sensitivity Genomic DNA kit. Libraries were prepared using the Ligation Sequencing gDNA - Native Barcoding Kit 24 V14 (SQK-NBD114.24) from Oxford Nanopore. Protocol was followed according to the manufacturer's guidelines with a starting material of 400 ng gDNA for each sample. The final pooled barcoded libraries were sequenced on GridION sequencer with a MinION flow cell (R10.4.1) for 24 hours continuously (GIGA Genomics Platform, Uliège).

Assembly was performed using the BV-BRC platform with Canu 1.7.1 and error correction by Racon v1.4.13. Assembled genomes were then annotated with RASTtk and aligned with Mauve v2.4.0 to compare differences. EasyFig v2.2.5 was used to compare capsular genomic regions. CRISPR spacer

were aligned on the K1-ULINTec4 genome using ClustalW Multiple alignment on BioEdit Sequence Alignment Editor v7.2.5.

2.10 Virulence assessment in *Galleria mellonella* larvae

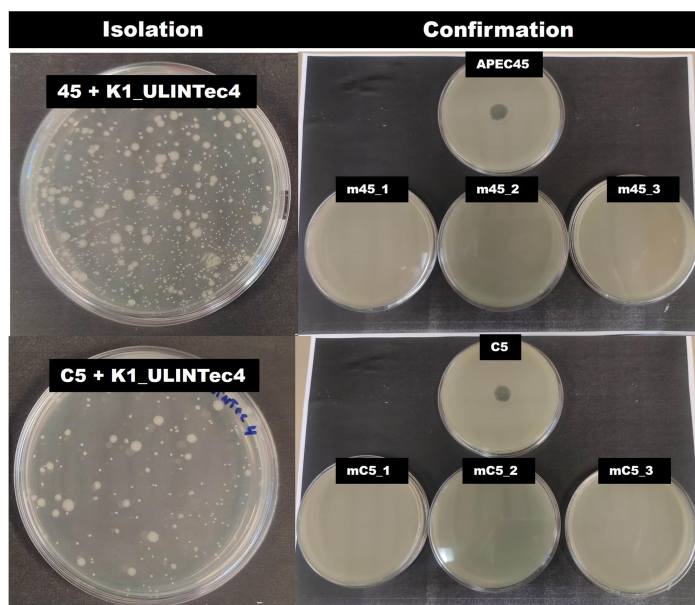
Virulence assessment was performed in *Galleria mellonella* larvae model for the six resistant isolates and the two sensitive strains. Nine groups of 30 larvae divided in 3 groups were inoculated using an automatic injector (Cole Parmer, Vernon Hills, IL, USA) with 10 µL of each strain (log 6 CFU/10µl) or PBS for the negative control. Each larva was inoculated in the last left proleg with a BD Plastipak™ 1mL sterile syringe (Becton-Dickinson, Franklin Lakes, NJ, USA) and a sterile 30-gauge needle (Terumo corporation, Tokyo, Japan). Larvae were incubated at 37 ° C and the mortality was evaluated every 24 hours for 4 days. The lethal doses (log 6 CFU/10µl) of strains APEC45 and C5 were selected following previous results (Antoine et al. 2023, Antoine et al. 2021). Kaplan-Meier survival curves were generated using GraphPad Prism version 8.0.2 for Windows, GraphPad Software (San Diego, CA, USA) and Logrank tests were performed to highlight any significant difference in survival rates between the groups ($p \leq 0.05$).

3. Results

3.1. Isolation of phage resistant mutants

Three colonies resistant to phage K1-ULINTec4 were harvested per strain: m45-1, m45_2, m45_3 and mC5_1, mC5_2, mC5_3. The colonies were selected as follows: one small-sized colony from the surface, one large-sized colony from the surface, and one from deep culture. All isolates were grown, and phage resistance was confirmed for each (**Figure 1**). The phage resistance of all isolates was stable after 10 passages.

226



227

228 **Figure 1.** Isolation and confirmation of phage resistant colonies from (up) APEC45 and (down) C5
 229 *Escherichia coli* strains. Spot tests of phage K1-ULINTec4 (4μL, 10⁹ PFU ml⁻¹) were used for
 230 confirmation of resistance.

231 3.2 Bacterial Growth Curves

232 APEC 45 and C5 strains, sensitive to phage K1-ULINTec4, showed growth after 5 hours of
 233 incubation. For the APEC 45 resistant mutants, the results showed no difference between the growth
 234 rates of the resistant strains, with or without phage, compared with the sensitive strain. For C5, results
 235 were similar except for strain m700973_2, which showed an inhibited growth in the presence and
 236 absence of phage K1-ULINTec4 (**Figure 2**).

237

ORIGINAL UNEDITED MANUSCRIPT

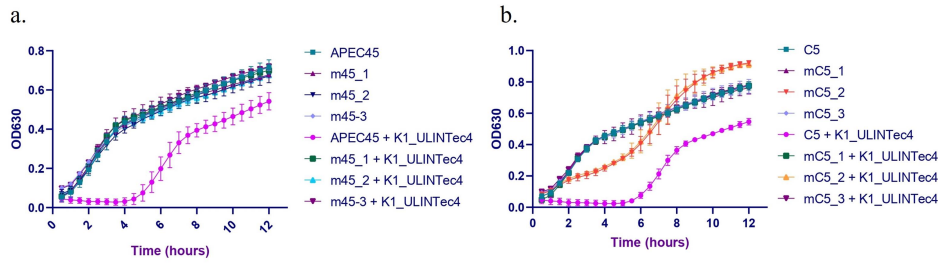


Figure 2. Growth curves of (a) APEC45, (b) C5 and phage resistant isolates with or without addition of phage K1-ULINTec4. OD: optical density (630nm)

3.3 Bacteriophage Adsorption

Adsorptions times were below 2 min for the sensitive strains (APEC45 and C5) and adsorption rates were $< 5 \times 10^{-7} \text{ mL}^{-1} \cdot \text{min}^{-1}$. Phage resistant strains never reached the 0.1 threshold before the end of the experiment (**Figure 3**).

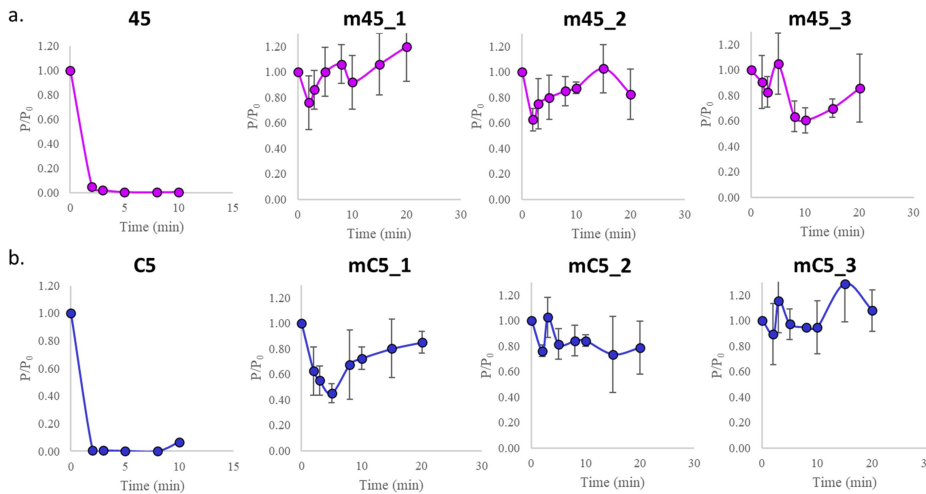


Figure 3. Phage adsorption curves of (a) sensitive and phage resistant (APEC45, m45_1, m45_2, m45_3) and (b) (C5, mC5_1, mC5_2 and mC5_3) isolates. P: number of free phages, P₀: initial phage concentration. The results represent the mean value of three titrations with standard deviation (SD).

3.4 Impact on Capsular production

To analyze a possible effect on the capsule, phenotypic tests were carried out, including the rapid K1 immunoassay and optical microscopy. The results for capsular K1 production were positive for both APEC 45 and C5. On the other hand, resistant isolates showed very weakly positive reaction (**Figure 4**)

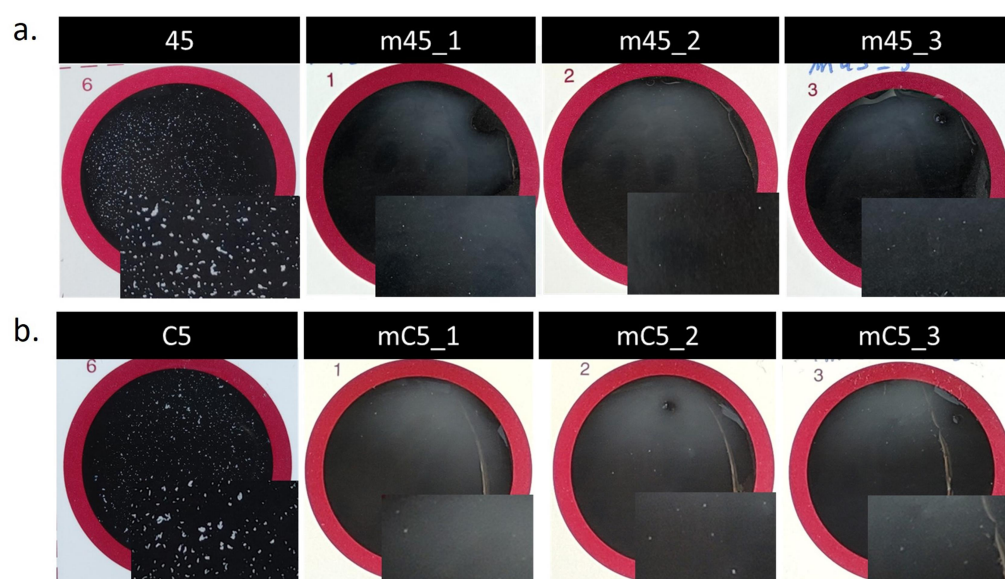


Figure 4. Pictures of the latex agglutination immunoassay revealing the presence of K1 capsular antigens, (a) sensitive and phage resistant (APEC45, m45_1, m45_2, m45_3) and (b) (C5, mC5_1, mC5_2 and mC5_3) isolates. A positive result produces small white agglutinations as showed for APEC45 and C5.

The negative staining shows the presence of capsules in both the sensitive (37°C) and resistant strains. However, the resistant strains are organized in small bacterial clusters, unlike the sensitive strains where the bacterial cells are isolated from each other (**Figure 5**). The presence of capsules contrast with the very low reaction to the K1 antigen observed in the immunoassay.

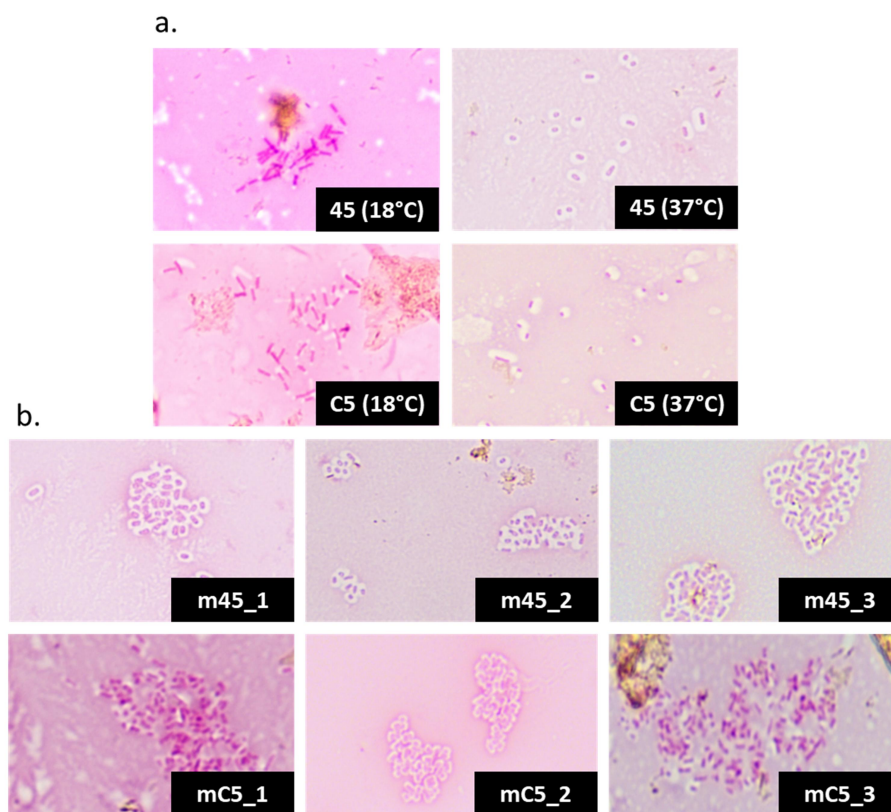


Figure 5. Microscopic images (x100) of (a) sensitive (APEC45 and C5) grown at 37°C and 18°C and (b) phage resistant (m45_1, m45_2, m45_3, mC5_1, mC5_2 and mC5_3) isolates grown at 37°C. Capsules are visible with negative Maneval staining (white halos around the bacteria).

3.5 Biofilm Production

Given the visualization of small bacterial clusters in microscopy, biofilm tests were carried out. The biofilms were all formed at the air-liquid interface of the wells. Biofilm production of phage-resistant isolates was significantly higher compared to the sensitive strains ($p < 0.0001$) (**Figure 6**).

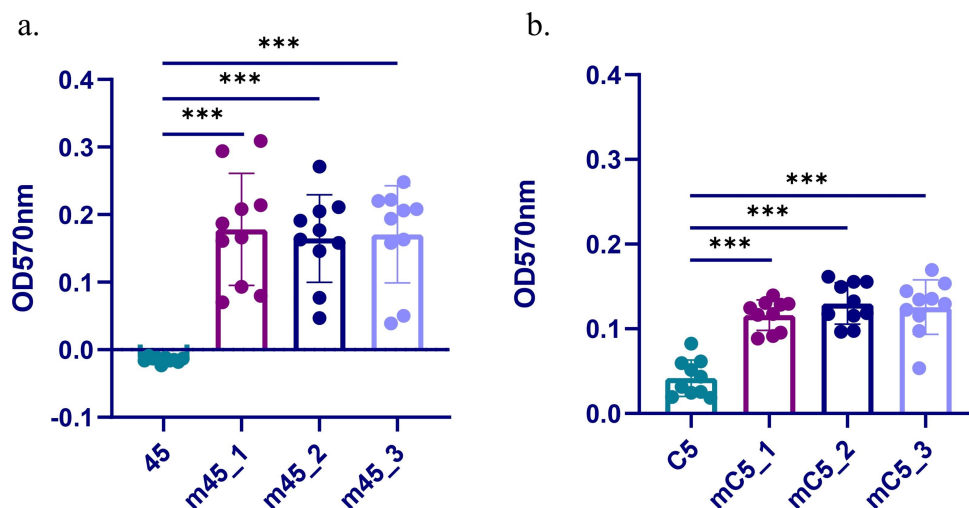
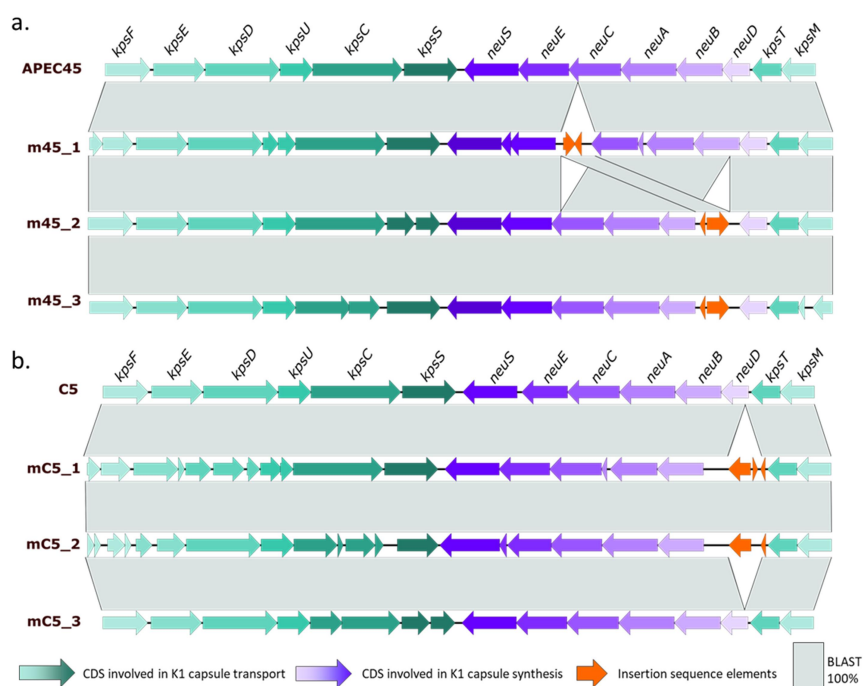


Figure 6. Quantification of the biofilm production (OD_{570nm}) of (a) APEC45 and phage resistant m45_1, m45_2, m45_3 and (b) C5, mC5_1, mC5_2, mC5_3. Results are presented as the mean of 10 replicates with SD. Statistical significance using one-way ANOVA with Dunnet's multiple comparison test is indicated as $p < 0.0001$ (***).

3.6 Genome analysis

In order to investigate any genetic modifications that may have led to phage resistance, a comparative genomic analysis was conducted. It revealed insertion sequences encoding IS1 protein InsA and IS1 protein InsB in the capsular region 2 of the *kps* cluster, involved in K1 capsule synthesis in all resistant isolates, except for mC5_3. These insertion sequences are located in different genes depending on the resistant isolates: *neuC*, *neuB* and *neuD* (**Figure 7**). The nucleotidic sequence of these insertions are similar between m45_1, m45_2 and m45_3 and between mC5_1 and mC5_2. These sequences differ depending on the origin (APEC45 or C5). Several disruptions in capsular genes are visible only in resistant strains. After alignment, these corresponded to mutations or indels. The existence of genes involved in the CRISPR-cas system has also been detected. The spacers were aligned with the genome of phage K1-ULINtec4 (accession number: MZ997839.1) but none matched the phage genome. Bacterial sequences were submitted as NCBI BioProject PRJNA1011853. Accession numbers are

294 **JAWMTB000000000** (APEC45), **JAWMSZ000000000** (m45_1), **JAWMTA000000000** (m45_2),
 295 **JAWMSU000000000** (m45_3), **JAWMSY000000000** (C5), **JAWMSV000000000** (mC5_1),
 296 **JAWMSX000000000** (mC5_2), **JAWMSW000000000** (mC5_3). Technical informations about
 297 sequences are available in supplementary file.



298

299

300 **Figure 7.** Capsular genes comparison of (a) APEC45 and phage resistant m45_1, m45_2, m45_3 and
 301 (b) C5, mC5_1, mC5_2, mC5_3. Coding sequence (CDS) involved in K1 capsule transport (green).
 302 CDS involved in K1 capsule synthesis (purple). Insertion sequence elements encoding IS1 protein
 303 InsA and IS1 protein InsB (orange).

304 3.7 *Galleria mellonella* Virulence Assessment

305 *Galleria* experiments were performed to assess the virulence of resistant isolates. Larvae injected with
 306 the APEC45 (log 6 CFU/10 μ L) strain showed 100% mortality after 96h, while for the C5 strain, the
 307 mortality reached 80% after the same time. Expected mortality was 100% and 90% respectively. In

comparison, the survival rates of larvae injected with phage-resistant isolates were all significantly better ($p < 0.0001$). No significant difference was found between resistant isolates. However, the survival rates of larvae in the control group (PBS) showed better survival than the resistant isolates: m45_1 ($p = 0.0115$), m45_2 ($p = 0.006$), m45_3 ($p = 0.0059$), mC5_1 ($p = 0.0124$), mC5_2 ($p = 0.0442$), mC5_3 ($p = 0.0116$). Kaplan–Meier survival curves are shown in **Figure 8**.

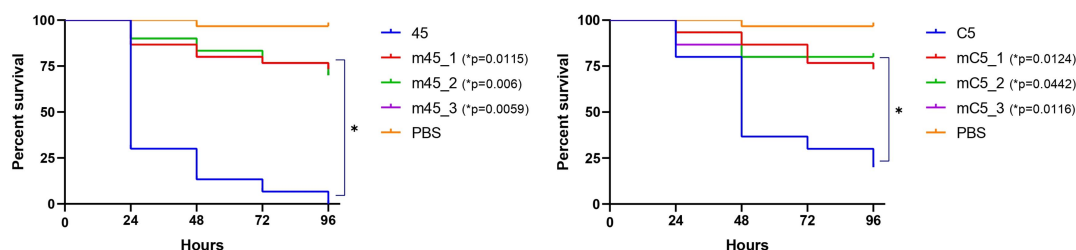


Figure 8. Kaplan–Meier survival curves of the experiments with *Galleria mellonella* larvae inoculated with (a) APEC45 and phage resistant m45_1, m45_2, m45_3 and (b) C5, mC5_1, mC5_2, mC5_3. Each group contained 30 larvae separated in 3 groups of 10 larvae. Log rank analysis showed significant increase in survival in all resistant isolates compared to the sensitive strain: m45_1 ($p = 0.0115$), m45_2 ($p = 0.006$), m45_3 ($p = 0.0059$), mC5_1 ($p = 0.0124$), mC5_2 ($p = 0.0442$), mC5_3 ($p = 0.0116$).

4. Discussion

Resistant colonies to phage K1-ULINtec4 were generated after the first contact with APEC45 and C5 bacteria respectively. The speed with which these resistances emerge can also be observed in the growth curves in liquid medium, with regrowth occurring five hours after contact with the phage. Moreover, growth of most resistant isolates showed no difference from controls in the presence or absence of the phage in the medium. Only mC5_2 showed a fitness cost demonstrated by a temporary growth inhibition with or without phage exposure. This is consistent with the results of two mutants produced in another study which linked this decrease in bacterial growth to a genomic mutation consisting of insertion sequences in respectively *neuC* and *kpsE* (Styles et al. 2022). Our results showed that these insertion sequences are present in genes *neuC*, *neuB* and *neuD* of the *kps* cluster,

even in isolates with unchanged growth which contrast with the study of Styles et al. 2022. No other genomic mutation was found in their study. Here, disruptions in other capsular genes have been identified only resistant isolates, corresponding to mutations or indels at nucleotide level. However, these results should be treated with caution, given the poorer base calling of nanopore sequencing. Short-read sequences could be used to confirm or refute this observation.

To study these resistances at the phenotypic level, several experiments were carried out, including adsorption times, antigenic detection of the K1 capsule and microscopic images. The results converged to a phage resistance mechanism related to receptor adaptation. The characteristic feature of bacterial resistance mechanisms linked to this mechanism is the modification, deletion or reduction of the phage receptor. Phage adsorption on resistant isolates was therefore evaluated, and it was found that the adsorption of K1-ULINTec4 was defective compared to controls. These findings are in line with the rapid immunoassay targeting the K1 capsule, which showed very weakly positive reactions on resistant isolates, indicating a significant impact on the capsular production. These results are also consistent with confocal microscopy results showing either absence or spatial reorganization of the capsular polysialic acid (PSA) in K1F resistant mutants (Styles et al. 2022). In contrast, our microscopic images obtained by negative Maneval staining showed that white halos similar to bacterial capsules were present, suggesting the possibility of a capsular modification that could decrease adsorption. In addition, the spatial organization of the bacteria was modified, and these were grouped into small clusters. Therefore, biofilm experiments were carried out to identify any biofilm production by resistant isolates. It has been demonstrated in several publications that phage resistance could lead to an increased biofilm production (Fernández et al. 2021, Hosseinidoust, Tufenkji and van de Ven 2013, Lacqua et al. 2006). Moreover it was demonstrated that the diffusion of soluble capsular polysaccharide into the surrounding environment by *E. coli* expressing group 2 capsules prevents the development of other bacteria (Valle et al. 2006). The results of the biofilm production tests were consistent with the microscopic images showing isolated bacteria for the sensitive strains and small bacterial clusters for the resistant strains. Biofilm production was significantly higher in resistant isolates. This consequence of phage resistance could pose challenges, particularly in the treatment of

urinary tract infections in which bacterial biofilms play an important role in pathogenesis (Sharma et al. 2016). Additionally, these biofilms might enhance the persistence of *E. coli* K1 in hospital environments, which is a major route of contamination for newborns, notably through the colonization of these bacteria in the nasogastric tubes (Alkeskas et al. 2015).

Experiments with APEC45 and C5 strains had already been carried out in the *Galleria mellonella* model to assess the safety and efficacy of phage K1-ULINtec4 (Antoine et al. 2021, Antoine et al. 2023). Larval survival was significantly increased following phage treatment. In addition, measurement of phage and bacterial concentrations in the model over 3 days revealed a possible resistance phenomenon, although this did not adversely affect survival (Antoine et al. 2021). In the present study, the results of in-vivo virulence assessment in the *G. mellonella* model showed improved survival of larvae infected with the resistant isolates compared to the sensitive APEC45 and C5 strains. This observation is consistent with previous research, in which targeted degradation of the PSA capsule on *E. coli* K1 strains resulted in altered phenotypes and reduced mortality in rat models (Mushtaq et al. 2004).

In conclusion, this study evaluated the development of resistance and the resulting phenotypic and virulence alterations in resistant isolates. As shown previously, even during rapid onset of resistance, elimination of the K1 capsule was able to decrease virulence in-vivo. However, the increase in biofilm production observed in phage resistant isolates could constitute an issue in the context of several infections including urinary tract infections and neonatal meningitis. This statement should be further evaluated specifically for each type of infection in order to assess its real impact.

377

Acknowledgments

We thank Jean-Noël Duprez for his technical support.

Conflicts of Interest: This work was performed in the context of a regionally funded project dedicated to the commercial development of bacteriophages as human medicines. A.F. is employed by FoodChain ID GENOMICS SA, and B.B. by Vésale Bioscience, which both participated in this project. The other authors declare no conflict of interest.

Funding

This work was supported by Wallonia in the framework of the call for projects organized by the BioWin competitiveness cluster.

Data Availability Statement: The data underlying this article are available in the article and in its online supplementary material.

References

- Alkeskas, Aldukali, Ogrodzki, Pauline, Saad, Mohamed, Masood, Naqash, Rhoma, Nasreddin R., Moore, Karen, et al., 'The Molecular Characterisation of Escherichia Coli K1 Isolated from Neonatal Nasogastric Feeding Tubes', *BMC Infectious Diseases*, 15/1 (2015)
<<http://dx.doi.org/10.1186/s12879-015-1210-7>>
- Antoine, Céline, Laforêt, Fanny, Blasdel, Bob, Fall, Abdoulaye, Duprez, Jean-Noël, Mainil, Jacques, et al., 'In Vitro Characterization and In Vivo Efficacy Assessment in Galleria Mellonella Larvae of Newly Isolated Bacteriophages against Escherichia Coli K1', *Viruses*, 13/10 (2021), 2005
- Antoine, Céline, Laforêt, Fanny, Goya-Jorge, Elizabeth, Gonza, Irma, Lebrun, Sarah, Douny, Caroline, et al., 'Phage Targeting Neonatal Meningitis E. Coli K1 In Vitro in the Intestinal Microbiota of Pregnant Donors and Impact on Bacterial Populations', *International Journal of Molecular Sciences*, 24/13 (2023), 10580
- Azam, Aa Haeruman, and Tanji, Yasunori, 'Bacteriophage-Host Arm Race: An Update on the Mechanism of Phage Resistance in Bacteria and Revenge of the Phage with the Perspective for Phage Therapy', *Applied Microbiology and Biotechnology*, 103/5 (2019), 2121–31
- Bull, J. J., Vimr, E. R., and Molineux, I. J., 'A Tale of Tails: Sialidase Is Key to Success in a Model of Phage Therapy against K1-Capsulated Escherichia Coli', *Bone*, 23/1 (2008), 1–7

- 409 Burmeister, Alita R., Fortier, Abigail, Roush, Carli, Lessing, Adam J., Bender, Rose G., Barahman,
410 Roxanna, et al., 'Pleiotropy Complicates a Trade-off between Phage Resistance and Antibiotic
411 Resistance', *Proceedings of the National Academy of Sciences*, 117/21 (2020), 11207–16
- 412 Chapman-McQuiston, E., and Wu, X. L., 'Stochastic Receptor Expression Allows Sensitive Bacteria
413 to Evade Phage Attack. Part I: Experiments', *Biophysical Journal*, 94/11 (2008), 4525–36
- 414 Dale, Adam P., and Woodford, Neil, 'Extra-Intestinal Pathogenic Escherichia Coli (ExPEC): Disease,
415 Carriage and Clones', *Journal of Infection*, 71/6 (2015), 615–26
- 416 Dy, Ron L., Przybilski, Rita, Semeijn, Koen, Salmond, George P.C., and Fineran, Peter C., 'A
417 Widespread Bacteriophage Abortive Infection System Functions through a Type IV Toxin–
418 Antitoxin Mechanism', *Nucleic Acids Research*, 42/7 (2014), 4590–4605
- 419 Dziva, Francis, and Stevens, Mark P., 'Colibacillosis in Poultry: Unravelling the Molecular Basis of
420 Virulence of Avian Pathogenic Escherichia Coli in Their Natural Hosts', *Avian Pathology*,
421 37/4 (2008), 355–66
- 422 Egidio, Julia E, Costa, Ana Rita, Aparicio-Maldonado, Cristian, Haas, Pieter-Jan, and Brouns, Stan J J,
423 'Mechanisms and Clinical Importance of Bacteriophage Resistance', *FEMS Microbiology*
424 *Reviews*, 46/1 (2022), fuab048
- 425 Fernández, Lucía, Gutiérrez, Diana, García, Pilar, and Rodríguez, Ana, 'Environmental pH Is a Key
426 Modulator of Staphylococcus Aureus Biofilm Development under Predation by the Virulent
427 Phage phiIPLA-RODI', *The ISME Journal*, 15/1 (2021), 245–59
- 428 Gencay, Yilmaz Emre, Sørensen, Martine C. H., Wenzel, Cory Q., Szymanski, Christine M., and
429 Brøndsted, Lone, 'Phase Variable Expression of a Single Phage Receptor in Campylobacter
430 Jejuni NCTC12662 Influences Sensitivity Toward Several Diverse CPS-Dependent Phages',
431 *Frontiers in Microbiology*, 9 (2018)
432 <<https://www.frontiersin.org/articles/10.3389/fmicb.2018.00082>> [accessed 18 September
433 2023]
- 434 Goldfarb, Tamara, Sberro, Hila, Weinstock, Eyal, Cohen, Ofir, Doron, Shany, Charpak-Amikam, Yoav,
435 et al., 'BREX Is a Novel Phage Resistance System Widespread in Microbial Genomes', *The*
436 *EMBO Journal*, 34/2 (2015), 169–83
- 437 Hosseinidoust, Zeinab, Tufenkji, Nathalie, and van de Ven, Theo G.M., 'Formation of Biofilms under
438 Phage Predation: Considerations Concerning a Biofilm Increase', *Biofouling*, 29/4 (2013),
439 457–68
- 440 KIM, KWANG SIK, 'Human Meningitis-Associated Escherichia Coli', *Physiology & Behavior*, 176/5
441 (2017), 139–48
- 442 Kim, Min Soo, Kim, Young Deuk, Hong, Sung Sik, Park, Kwangseo, Ko, Kwan Soo, and Myung,
443 Heejoon, 'Phage-Encoded Colanic Acid-Degrading Enzyme Permits Lytic Phage Infection of
444 a Capsule-Forming Resistant Mutant Escherichia Coli Strain', *Applied and Environmental*
445 *Microbiology*, 81/3 (2015), 900–909
- 446 King, Jane E., Aal Owaif, Hasan A., Jia, Jia, and Roberts, Ian S., 'Phenotypic Heterogeneity in
447 Expression of the K1 Polysaccharide Capsule of Uropathogenic Escherichia Coli and
448 Downregulation of the Capsule Genes during Growth in Urine', *Infection and Immunity*, 83/7
449 (2015), 2605–13
- 450 Lacqua, Andrea, Wanner, Oskar, Colangelo, Teresa, Martinotti, Maria Giovanna, and Landini, Paolo,
451 'Emergence of Biofilm-Forming Subpopulations upon Exposure of Escherichia Coli to

- 452 Environmental Bacteriophages', *Applied and Environmental Microbiology*, 72/1 (2006), 956–
453 59
- 454 Leiman, Petr G., Battisti, Anthony J., Bowman, Valorie D., Stummeyer, Katharina, Mühlenhoff,
455 Martina, Gerardy-Schahn, Rita, et al., 'The Structures of Bacteriophages K1E and K1-5
456 Explain Processive Degradation of Polysaccharide Capsules and Evolution of New Host
457 Specificities', *Journal of Molecular Biology*, 371/3 (2007), 836–49
- 458 Maneval, W. E., 'Staining Bacteria and Yeasts with Acid Dyes', *Stain Technology*, 2009
459 <<https://www.tandfonline.com/doi/abs/10.3109/10520294109106189>> [accessed 14 August
460 2023]
- 461 Mangalea, Mihnea R., and Duerkop, Breck A., 'Fitness Trade-Offs Resulting from Bacteriophage
462 Resistance Potentiate Synergistic Antibacterial Strategies', *Infection and Immunity*, 88/7
463 (2020), e00926-19
- 464 McCarthy, Alex J., Birchenough, George M. H., and Taylor, Peter W., 'Loss of Trefoil Factor 2
465 Sensitizes Rat Pups to Systemic Infection with the Neonatal Pathogen Escherichia Coli K1',
466 *Infection and Immunity*, 87/5 (2019), e00878-18
- 467 McCarthy, Alex J., Negus, David, Martin, Patricia, Pechincha, Catarina, Oswald, Eric, Stabler, Richard
468 A., et al., 'Pathoadaptive Mutations of Escherichia Coli K1 in Experimental Neonatal
469 Systemic Infection', *PLoS ONE*, 11/11 (2016), 1–16
- 470 Millen, Anne M., Horvath, Philippe, Boyaval, Patrick, and Romero, Dennis A., 'Mobile CRISPR/Cas-
471 Mediated Bacteriophage Resistance in Lactococcus Lactis', *PLOS ONE*, 7/12 (2012), e51663
- 472 Møller-Olsen, Christian, Ho, Siu Fung Stanley, Shukla, Ranti Dev, Feher, Tamas, and Sagona, Antonia
473 P., 'Engineered K1F Bacteriophages Kill Intracellular Escherichia Coli K1 in Human
474 Epithelial Cells', *Scientific Reports*, 8/1 (2018), 17559
- 475 Mora, Azucena, Viso, Susana, López, Cecilia, Alonso, María Pilar, García-Garrote, Fernando, Dabhi,
476 Ghizlane, et al., 'Poultry as Reservoir for Extraintestinal Pathogenic Escherichia Coli
477 O45:K1:H7-B2-ST95 in Humans', *Veterinary Microbiology*, 167/3 (2013), 506–12
- 478 Moulin-Schouleur, Maryvonne, Schouler, Catherine, Tailliez, Patrick, Kao, Mu Rong, Brée, Annie,
479 Germon, Pierre, et al., 'Common Virulence Factors and Genetic Relationships between
480 O18:K1:H7 Escherichia Coli Isolates of Human and Avian Origin', *Journal of Clinical
481 Microbiology*, 44/10 (2006), 3484–92
- 482 Mushtaq, Naseem, Redpath, Maria B., Luzio, J. Paul, and Taylor, Peter W., 'Prevention and Cure of
483 Systemic Escherichia Coli K1 Infection by Modification of the Bacterial Phenotype',
484 *Antimicrobial Agents and Chemotherapy*, 48/5 (2004), 1503–8
- 485 Ofir, Gal, Melamed, Sarah, Sberro, Hila, Mukamel, Zohar, Silverman, Shahar, Yaakov, Gilad, et al.,
486 'DISARM Is a Widespread Bacterial Defence System with Broad Anti-Phage Activities',
487 *Nature Microbiology*, 3/1 (2018), 90–98
- 488 Oliveira, Pedro H., Touchon, Marie, and Rocha, Eduardo P.C., 'The Interplay of Restriction-
489 Modification Systems with Mobile Genetic Elements and Their Prokaryotic Hosts', *Nucleic
490 Acids Research*, 42/16 (2014), 10618–31
- 491 Sarowska, Jolanta, Futoma-Koloch, Bozena, Jama-Kmiecik, Agnieszka, Frej-Madrzak, Magdalena,
492 Ksiazczyk, Marta, Bugla-Ploskonska, Gabriela, et al., 'Virulence Factors, Prevalence and
493 Potential Transmission of Extraintestinal Pathogenic Escherichia Coli Isolated from Different
494 Sources: Recent Reports', *Gut Pathogens*, 11/1 (2019), 1–16

- 495 Schneider, György, Szentes, Nikolett, Horváth, Marianna, Dorn, Ágnes, Cox, Alysia, Nagy, Gábor, et
496 al., 'Kinetics of Targeted Phage Rescue in a Mouse Model of Systemic Escherichia Coli K1',
497 *BioMed Research International*, 2018 (2018)
- 498 Scholl, D., Rogers, S., Adhya, S., and Merrill, C. R., 'Bacteriophage K1-5 Encodes Two Different Tail
499 Fiber Proteins, Allowing It To Infect and Replicate on Both K1 and K5 Strains of Escherichia
500 Coli', *Journal of Virology*, 75/6 (2001), 2509–15
- 501 Seed, Kimberley D., Faruque, Shah M., Mekalanos, John J., Calderwood, Stephen B., Qadri, Firdausi,
502 and Camilli, Andrew, 'Phase Variable O Antigen Biosynthetic Genes Control Expression of
503 the Major Protective Antigen and Bacteriophage Receptor in Vibrio Cholerae O1', *PLoS*
504 *Pathogens*, 8/9 (2012), e1002917
- 505 Sharma, G., Sharma, S., Sharma, P., Chandola, D., Dang, S., Gupta, S., et al., 'Escherichia Coli
506 Biofilm: Development and Therapeutic Strategies', *Journal of Applied Microbiology*, 121/2
507 (2016), 309–19
- 508 Smith, H. Williams, and Huggins, M. B., 'Successful Treatment of Experimental Escherichia Coli
509 Infections in Mice Using Phage: Its General Superiority over Antibiotics', *Microbiology*,
510 128/2 (1982), 307–18
- 511 Styles, Kathryn M., Locke, Rebecca K., Cowley, Lauren A., Brown, Aidan T., and Sagona, Antonia P.,
512 'Transposable Element Insertions into the Escherichia Coli Polysialic Acid Gene Cluster
513 Result in Resistance to the K1F Bacteriophage', *Microbiology Spectrum*, 10/3 (2022), e02112-
514 21
- 515 Valle, Jaione, Da Re, Sandra, Henry, Nelly, Fontaine, Thierry, Balestrino, Damien, Latour-Lambert,
516 Patricia, et al., 'Broad-Spectrum Biofilm Inhibition by a Secreted Bacterial Polysaccharide',
517 *Proceedings of the National Academy of Sciences of the United States of America*, 103/33
518 (2006), 12558–63
- 519 Wu, Jin'en, Yang, Jing, Cho, William C., and Zheng, Yadong, 'Argonaute Proteins: Structural
520 Features, Functions and Emerging Roles', *Journal of Advanced Research*, 24 (2020), 317–24
- 521
- 522

523

524 **Author Contributions:** Conceptualization, C.A., D.T. and V.D.; methodology, C.A., D.T. and V.D.;
525 software, C.A, B.B and A.F.; validation, C.A., F.L.; formal analysis, C.A., D.T.; investigation, C.A.,
526 D.T., F.L., B.B. and A.F.; resources, D.T. and V.D.; data curation, F.L. and B.B.; writing—original
527 draft preparation, C.A.; writing—review and editing, C.A., F.L, A.F., B.B., V.D. and D.T.;
528 visualization, C.A.; supervision, D.T. and V.D.; project administration, D.T. and V.D.; funding
529 acquisition, D.T. and V.D. All authors have read and agreed to the published version of the manuscript.

530

ORIGINAL UNEDITED MANUSCRIPT